JOURNAL OF COMPUTATIONAL PHYSICS 38, 45–63 (1980)

An Orbit Averaged Particle Code*

BRUCE I. COHEN, THOMAS A. BRENGLE,
DAVIS B. CONLEY, AND ROBERT P. FREIS

Lawrence Livermore Laboratory, University of California,
Livermore, California 94550

Received June 20, 1979

A new method for efficient computer simulation of long time-scale plasma physics phenomena is proposed which has proved successful in one- and two-dimensional magneto-inductive particle codes. The method relies on orbit-averaging charge and current densities in Maxwell's equations before solving for the self-consistent electric and magnetic fields in order to filter out unwanted high-frequency oscillations and reduce the number of simulation particles necessary to fill phase space adequately. This method offers the potential of greatly improving the economics of simulating the evolution of a plasma over time intervals which are long compared to particle orbit periods. A particular scheme using a predictor–corrector iterative method and time splitting is discussed, which is both stable and accurate. Application to the efficient simulation of a magnetic mirror machine plasma injected with energetic neutral beams is presented.

1. INTRODUCTION

The efficient simulation of collective plasma behavior is made extremely difficult by the large range in magnitude of both spatial and temporal scales over which interesting physics occurs in laboratory and natural plasma. The success in recent years of the particle approach to computer simulation of plasmas is due in great part to gains made in reducing the range of space scales present in simulations by intelligent use of grids, finite-sized particles, and spatial smoothing and filtering techniques [1]. A hybrid simulation technique, in which a combination of fluid and particle equations is used, has been useful in reducing or eliminating both noise due to particle discreteness and unwanted high-frequency oscillations. A couple of examples of hybrid codes are described in Ref. [2]. However, the elimination of fast time-scale

581/38/1-4 0021-9991/80/130045–19$02.00/0

phenomena in this type of simulation is necessarily accompanied by the loss of kinetic effects. In this work we wish to retain kinetic effects arising from the particle orbits, e.g., finite Larmor-radius effects, but remove high-frequency oscillations in electric and magnetic fields, and follow only relatively slower variations.

This article describes the introduction and use of a new method for particle simulation of plasmas, which follows individual particles over their natural time scale, but which solves Maxwell's equations for the self-consistent electric and magnetic fields relatively less often as they vary over a much longer time scale. Byers suggested that a conventional particle code, one that solved for fields as often as it advanced particle velocities and positions, could be extended to simulations of very slowly varying phenomena by some means of temporally averaging or filtering the plasma current and charge densities appearing as sources in Maxwell's equations [3]. The goal was to reduce the requirements on the number of particles necessary for accurate, reproducible, and quiet simulations and hence also to reduce the ultimate computer memory requirement and run-time of a typical simulation. In this simulation scheme any given particle would fill in a relatively larger region of phase between successive solutions of the field equations. A similar idea has been used in simulations which calculated self-consistent steady-state electric fields for a set of representative particle trajectories [4]. If orbit averaging could be done in a time-dependent simulation without sacrifice of numerical stability and accuracy, then simulation of relatively slowly developing plasma phenomena with this technique might require much less in computer resources than would more conventional approaches. For example, this could make feasible large SUPERLAYER simulations [5] of build-up of a magnetic-mirror fusion plasma approaching reversal of the magnetic field using parameters closely modeling mirror experiments at Lawrence Livermore Laboratory. This is in fact our most immediate goal.

The idea of splitting the solving of the particle equations of motion and the field equations is not new; it has been used in particle codes, and some of its aspects have been analyzed in previous investigations [6, 7]. Godfrey analyzed the conditions for numerical Cherenkov instabilities in electromagnetic codes in which particle quantities were advanced for N time steps ($N \geqslant 1$) before the current was accumulated and the field equations were solved [6]. However, there was no temporal averaging of the current in the algorithms he considered. His results indicated that numerical stability worsened as N increased, but he overlooked a virulent numerical instability associated with temporal aliasing when $N > 1$. Langdon and Lasinski observed this instability in some of their simulations [7].

The extension of plasma simulation algorithms to longer time steps has received a great deal of attention in recent years. The methods introduced by Denavit and his co-workers in this area have been especially imaginative and creative [8, 9]. Rathmann, Vomvoridis, and Denavit introduced in Ref. [8] a hybrid simulation scheme in which particles are advanced with long time steps, $\Delta t \gg \omega_p^{-1}, \omega_c^{-1}$, where ω_p and ω_c are plasma and cyclotron frequencies, which are limited only by a relatively slow nonlinear time scale. This was achieved by decomposition of the fields into a limited number of spatial Fourier modes and linearization of the particle equa-

tions of motion with respect to the fields. Crystal, Denavit, and Rathmann have more recently explored the extension of fluid or Vlasov simulations to longer time steps by implicit solution of difference equations [9]. Their algorithms require inversion of sparse matrices which can be done accurately and efficiently. On the other hand, Langdon [10] has pointed out in a general analysis of finite time-step considerations in particle codes certain fundamental difficulties that preclude some approaches to large Δt.

We have taken a *new* point of view on the long time-step problem. We combine time-splitting with temporal averaging to allow the self-consistent solution of Maxwell's equations on a slow time scale using a long time step, but we insist that the particle dynamics be followed on the natural time scale of the orbit. (We should comment on our use of the words "temporal averaging" or "orbit-averaging." A weighted normalized sum of the plasma currents over a long time interval is computed in our code before Maxwell's equations are solved for the electromagnetic fields. We describe this weighted sum as a temporal or orbit average. However, only values of the plasma currents which have already been determined by either a predictor or corrector projection of the particle orbits are used. This scheme is discussed in detail in Section 3.) In the cases of interest to us here, the particle orbit time scale is set by the cyclotron frequency associated with an externally applied magnetic field. This is typically much faster than the time scales for plasma transport and on which self-consistent electric and magnetic fields in the plasma vary due to, for example, neutral-beam injection or radio-frequency heating at low frequency. In Section 2 we introduce a specific physics model to which we have applied orbit-averaging. We also present a simplified analysis of the impact of orbit-averaging on the dispersion relation for the linear normal modes in this model. This has provided useful intuition and has motivated certain features in our algorithms. A specific algorithm combining orbit-averaging and time-splitting in a magneto-inductive simulation [5, 11, 12] is described in Section 3. We report the results of simulations in Section 4.

2. Analysis of Model Equations

Motivated by the desire to simulate the build-up of a mirror plasma by neutral-beam injection to high β, $\beta \equiv 4\pi nm\langle v^2\rangle/B^2$, and reversal of the magnetic field, we consider the one- and two-dimensional magneto-inductive particle codes MAGIC [12] and SUPERLAYER [5]. These codes use a Darwin model [13] to calculate self-consistent electric and magnetic fields from the plasma currents provided by finite-orbit ions, assume charge neutrality, and neglect electrostatic fields and electron dynamics (appropriate assumptions for open magnetic field lines, $T_i \gg T_e$, and slowly varying phenomena: $|\partial/\partial t| \leqslant \omega_{ci}^0 \equiv eB_0/m_i c$). A schematic of the coordinate system and variables in the one-dimensional, cylindrically symmetric code MAGIC is shown in Fig. 1.

MAGIC employs a conventional Boris pusher for advancing particle velocities and positions [14]. A cloud-in-cell particle representation is used [15]. The particle

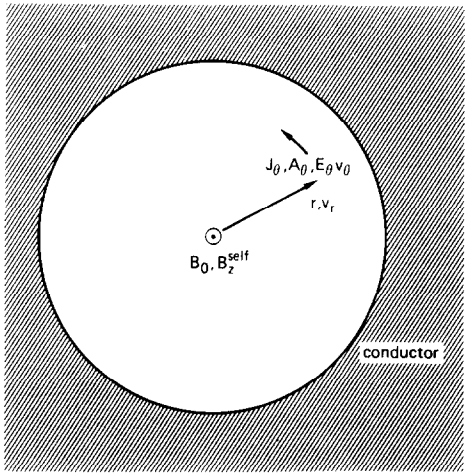

FIG. 1. Coordinate scheme and variables for one-dimensional, cylindrically symmetric, magneto-inductive particle simulation.

current J_θ is accumulated on a uniformly spaced radial grid by means of linear interpolation. A simulation particle occupies a cylinder of radius r, width Δr, and unit length in z; hence, particle charge and current densities must be normalized to a volume $2\pi r\Delta r$, which is not necessarily constant in time. Once the plasma current is known, Ampère's law determines the self-consistent magnetic field B_z with the displacement current neglected. Faraday's law then gives the induction electric field E_θ associated with any changes in the magnetic field. With the self-consistent electric and magnetic fields, the particle velocities (v_θ, v_r) and radial positions r can then be advanced to their new values. The particle and field equations fit together in the usual leap-frog fashion [1, 12].

To illustrate the influence of temporally averaging the current J_θ on the linear normal modes of the simulation model, we now present a simple model analysis in slab geometry ($\theta \to y$, $r \to x$). However, this analytical model does not split the time scales for calculating fields and particle orbits. We ignore spatial grid effects and only analyze the effects of finite time step. The model difference equations are

$$(D_x^2)_j \frac{1}{2}(A_y^{n+1} + A_y^n) = \frac{-4\pi}{c} \sum_{n'} W(n-n') J_{y,j}^{n'+1/2} \tag{1}$$

$$\frac{1}{2}(E_y^{n+1} + E_y^n)_j = -\frac{1}{c\Delta t}(A_y^{n+1} - A_y^n)_j \tag{2}$$

$$B_{z,j}^n = B_0 + D_{x,j} A_y^n \tag{3}$$

$$v_x^{n+1/2} = v_x^{n-1/2} + \sum_j \frac{e\Delta t}{2mc} S(x^n - x_j)(v_y^{n+1/2} + v_y^{n-1/2}) B_{z,j}^n \tag{4}$$

$$v_y^{n+1/2} = v_y^{n-1/2} + \sum_j \frac{e\Delta t}{m} S(x^n - x_j)\left[E_{y,j}^n - \frac{1}{2c}(v_x^{n+1/2} + v_x^{n-1/2})B_{z,j}^n\right] \quad (5)$$

$$x^{n+1} = x^n + v_x^{n+1/2}\Delta t, \quad (6)$$

where $S(x^n - x_j)$ is the usual interpolation factor accounting for finite-sized particles and a discrete spatial grid [1]; j is the spatial grid index; B_0 is a uniform applied magnetic field, $D_{x,j}$ and $(D_x^2)_j$ are the standard centered two-point and three-point first and second spatial difference operators; n denotes the time level; and W is the data window or, more formally, a normalized digital-smoothing function, $\sum_{n'} W(n - n') = 1$. Thus, on the right side of Eq. (1) a weighted time-average of J_y is calculated. We construct J_y using

$$J_{y,j}^{n+1/2} = \sum_i \frac{e}{2}[S(x_i^n - x_j) + S(x_i^{n+1} - x_j)]v_{y,i}^{n+1/2} \quad (7a)$$

or

$$J_{y,j}^n = \sum_i \frac{eS(x_i^n - x_j)}{m}\left[P_{y,i} - \frac{e}{c}B_0 x_i^n - \frac{e}{c}\sum_{j'} S(x_i^n - x_{j'})A_{y,j'}^n\right], \quad (7b)$$

where $P_y \equiv mv_y + eB_0 x/c + e\sum_j S(x - x_j)\,A_{y,j}/c$ is the canonical momentum and is conserved in this model. Because the current J_y is given in Eq. (7b) at integer time steps, the left side of Eq. (1) is replaced with $(D_x^2)_j A_y^n$ when Eq. (7b) is employed; and Eq. (1) determines A_y^n implicitly.

At this point we examine the propagation of small amplitude waves that are admitted by these model equations in the limit of a cold plasma. We linearize Eqs. (1) to (7), Fourier transform in time, ignore temporal aliasing [1, 10], and set $\Delta x = 0$. For the model that constructs the current J_y directly from the particle velocities v_y, Eq. (7a), the relevant Fourier-transformed difference equations are

$$-k_x^2 \tilde{A}_y \cos \omega\Delta t/2 = -4\pi n_0 e c^{-1}\,\tilde{W}(\omega)\tilde{v}_y \quad (8a)$$

$$\tilde{E}_y \cos \omega\Delta t/2 = i\tilde{A}_y(c\Delta t/2)^{-1} \sin \omega\Delta t/2 \quad (8b)$$

$$-i\tilde{v}_x \sin \omega\Delta t/2 = (\omega_c^0\,\Delta t/2)\tilde{v}_y \cos \omega\Delta t/2 \quad (8c)$$

$$-i\tilde{v}_y \sin \omega\Delta t/2 = (e\Delta t/2m)\tilde{E}_y - (\omega_c^0\,\Delta t/2)\tilde{v}_x \cos \omega\Delta t/2, \quad (8d)$$

where $\omega_c^0 \equiv eB_0/mc$ and n_0 is the plasma density.

Algebraic reduction of this system of equation is straightforward: we obtain the dispersion relation

$$\tilde{W}Y^2 + (\tilde{W} + k_x^2 c^2/\omega_{pi}^2)Y - k_x^2 v_A^2\,\Delta t^2/4 = 0, \quad (9)$$

where $v_A \equiv \omega_c^0 c/\omega_p$ is the Alfvén velocity and $Y \equiv \tan^2(\omega\Delta t/2)$. To follow accurately

the cyclotron motion, one must require that $\omega_c^0 \Delta t \ll 1$. In this limit the two solutions of Eq. (9) are given by

$$Y = \frac{k_x^2 v_A^2 \Delta t^2/4}{\tilde{W} + k_x^2 c^2/\omega_p^2} \tag{10a}$$

and

$$Y = -(1 + k_x^2 c^2/\tilde{W}\omega_p^2). \tag{10b}$$

The first solution, Eq. (10a), is the compressional Alfvén branch. For $\tilde{W} \geqslant 0$, these waves are unconditionally stable; and $Y \leqslant \omega_c^2 \Delta t^2/4$. When $\tilde{W} = 0$, $\tilde{A}_y$ and $\tilde{E}_y$ are consequently zero; and simple cyclotron oscillations of $\tilde{v}_x$ and $\tilde{v}_y$ are recovered from Eqs. (8c) and (8d) with frequency described by Eq. (10a). Thus, the spectrum of Alfvén waves can be modified and filtered by suitable choice of digital-smoothing function $W(t)$.

The remaining solution of Eq. (9), Eq. (10b), describes unstable even–odd oscillations. The source of even–odd oscillations is the identical time-centering and simple averaging of the left sides of Eqs. (1) and (2). We can partially compensate for this difficulty by slightly uncentering Eqs. (1) and (2):

$$\begin{aligned} &(D_x^2)_j \tfrac{1}{2}(A_y^{n+1} + A_y^n) \to (D_x^2)_j [\alpha A_y^{n+1} + (1-\alpha) A_y^n] \\ &\tfrac{1}{2}(E_y^{n+1} + E_y^n)_j \to [\eta E_y^{n+1} + (1-\eta) E_y^n]_j. \end{aligned} \tag{11}$$

We introduce frequency-dependent dissipation with choice of α and η such that α, $\eta > \frac{1}{2}$. Equations (1) and (2) are then biased in the backward direction. We have confirmed the dissipative effect of α, $\eta > \frac{1}{2}$ with analysis and simulations for $W(n-n') = 1$ when $n = n'$ and zero otherwise, which corresponds to no time-averaging. For this case the damping rate of a particular mode is proportional to $(\alpha + \eta - 1)\omega^2 \Delta t$.

For an algorithm employing the representation of J_y given by Eq. (7b), there is only the compressional Alfvén branch:

$$\tan^2(\omega \Delta t/2) = \frac{k_x^2 v_A^2 \Delta t^2/4}{[1 + (\omega_c^0 \Delta t/2)^2]\tilde{W} + k_x^2 c^2/\omega_p^2}. \tag{12}$$

These modes are unconditionally stable for $\tilde{W} \geqslant 0$. When $\tilde{W} = 0$, $\tilde{E}_y$ and $\tilde{A}_y$ are completely damped; only cyclotron oscillations of the particle velocities and positions persist. For $\tilde{W} > 0$ and $\omega_c^0 \Delta t/2 \gg 1$, very short wavelength modes are folded back down in frequency into *stable* even–odd oscillations $\omega \Delta t = \pm\pi$ (see Fig. 2). For $\tilde{W} = 1$ and $\omega_c^0 \Delta t/2 \ll 1$, $\omega^2 \Delta t^2/4 \leqslant \tan^2(\omega \Delta t/2) \leqslant \omega_c^{0^2} \Delta t^2/4 \ll 1$; and the compressional Alfvén branch is stable and suffers very little numerical dispersion. The code MAGIC [12] takes advantage of the stability of this algorithm, but performs no time-averaging ($\tilde{W} = 1$).

The analysis presented in this section has established the numerical dispersion and

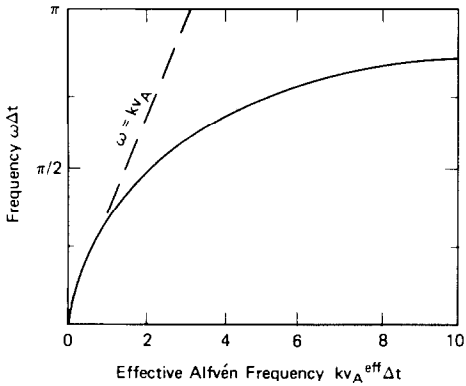

FIG. 2. Dispersion relation for compressional Alfvén waves in a model orbit-averaged magneto-inductive algorithm for $\tilde{W}_\omega \geqslant 0$ and $\omega_{ci}^0 \Delta t \gg 1$. The effective Alfvén frequency is given by $kv^{\text{eff}} \equiv kv_A/\{[1+(\omega_{ci}^0\Delta t/2)^2]\tilde{W} + k^2c^2/\omega_{pi}^2\}^{1/2}$ for the algorithm using Eq. (7b). For $\tilde{W}_\omega \geqslant 0$ and $\omega_{ci}^0 \Delta t < 1$, $|\omega| \leqslant \omega_{ci}^0$.

dissipation characteristics of the compressional Alfvén waves admitted by a magneto-inductive simulation model. The main conclusion is that the model algorithm employing canonical momentum ought to be more stable than the one relating the transverse current directly to the particle velocities. Orbit-averaging modifies the spectrum of waves exhibited. With appropriate shaping of the filtering function W, the numerical dispersion added to low-frequency waves can be minimized and high-frequency waves outside the bandwidth of the filter can be quite effectively damped. Uncentering of Maxwell's equations can add frequency-dependent dissipation, which we find useful in controlling numerical instability and errors. The model algorithm analyzed in this section has been employed in the code MAGIC only in the limit of no orbit-averaging ($\tilde{W}_\omega = 1$). We have not implemented any of the more general class of algorithms with $\tilde{W}_\omega \neq 1$ except as combined with time-splitting of the particle and field equations (discussed in Sections 3 and 4). Nevertheless, our analysis establishes intuition for some of the numerical characteristics and simple types of waves expected in the simulation scheme described in the next section.

3. ORBIT-AVERAGED MAGNETO-INDUCTIVE ALGORITHM

We have added orbit-averaging and time-splitting to the SUPERLAYER [5] and MAGIC [12] algorithms and given the new codes the names SUPERAVERAGE and MAGICL. Both codes have the following computational scheme illustrated in Fig. 3. Electric and magnetic fields **E** and **B** are determined at discrete macro time steps ΔT. The particle motion is calculated incrementally at micro time steps Δt, $\Delta t \ll \Delta T$. The computational cycle begins with fields given at the last macro time step (or at $t = 0$ for the first time step). Particle velocities and positions are then advanced over many

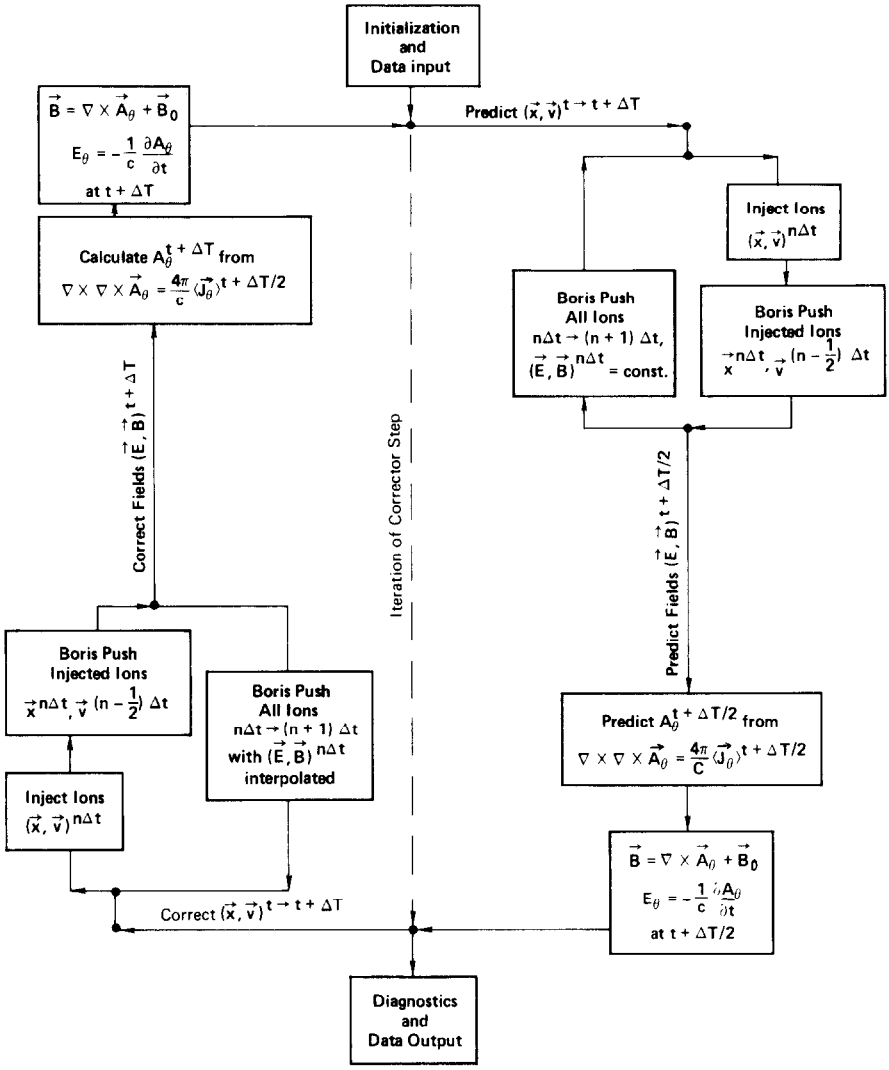

FIG. 3. Block diagram for the orbit-averaged codes MAGICL and SUPERAVERAGE.

micro time steps with **E** and **B** fixed. The canonical form of the equations of motion used is given by

$$\mathbf{v}^{n+1/2} = \mathbf{v}^{n-1/2} + \sum_j (e/m)\,\Delta t\, S(r^n - r_j)\left[\mathbf{E}_j + \frac{1}{2c}(\mathbf{v}^{n+1/2} \times \mathbf{B}_j + \mathbf{v}^{n-1/2}) - \frac{m}{2e} v_j^{i/e}(\mathbf{v}^{n+1/2} + \mathbf{v}^{n-1/2})\right] \tag{13a}$$

and

$$r^{n+1} = [(r^n + v_r^{n+1/2}\,\Delta t)^2 + (v_\theta^{n+1/2}\,\Delta t)^2]^{1/2}, \tag{13b}$$

where j is the spatial grid index, $\nu_j^{i/e}$ is the spatially dependent ion-electron drag rate, and solutions of Eqs. (13a) and (13b) for $\mathbf{v}^{n+1/2}$ and r^{n+1} follow Boris' scheme with finite $\omega_c \Delta t$ corrections included [14].

The transverse current J_θ is accumulated on a radial grid at each micro time step according to one of the following prescriptions,

$$J_{\theta,j}^{n+1/2} = \frac{e}{2} \sum_i [S(r_i^n - r_j) v_{\theta,i}^{n+1/2} + S(r_i^{n+1} - r_j) v_{\theta,i}^{n+1/2}] \tag{14a}$$

or

$$\begin{aligned} J_{\theta,j}^n &= \frac{e}{m} \sum_i \frac{S(r_i^n - r_j)}{r_i^n} \left[L_{\theta,i} - \frac{e}{c} \sum_l S(r_i^n - r_l)\psi_l \right] \\ &\approx \frac{e}{m} \sum_i \frac{S(r_i^n - r_j)}{r_i^n} \left[L_{\theta,i} - \frac{e}{c}\psi_j \right], \end{aligned} \tag{14b}$$

where $L_{\theta,i}$ is the canonical angular momentum of the ith particle and $\psi \equiv rA_\theta$ is related to the magnetic flux. The use of $L_{\theta,i}$ in Eq. (14b) requires an additional storage array. In Eq. (14a) the first factor $v_{\theta,i}^{n+1/2}$ appearing is relative to the particle position vector $\mathbf{r}_i^n$, while the second $v_{\theta,i}^{n+1/2}$ is relative to $\mathbf{r}_i^{n+1}$ (see Ref. [14]).

The approximation made on the right side of Eq. (14b) simplifies the computations without apparent deleterious effect on our simulations. There is a certain small loss of momentum conservation due to the existence of a fictitious self-force connected with this approximation [15]. However, good particle statistics per spatial cell and the absence of significant variations of the particle density over a cell justify the replacement,

$$S(r_i^n - r_j) \sum_l S(r_i^n - r_l)\psi_l \approx S(r_i^n - r_j) \sum_l S(r_i^n - r_l)\psi_j = S(r_i^n - r_j)\psi_j,$$

which has been made in Eq. (14b). The computational gain due to this approximation and the basis for its adequacy were previously pointed out by Dickman, Morse, and Nielson [11].

The algorithm next calculates the magnetic flux $\psi \equiv rA_0$ from Ampère's law

$$\begin{aligned} \left(\frac{\partial^2}{\partial r^2} - \frac{1}{r^2} \right)_j \frac{\psi^{M+1/2}}{r} &= -\frac{4\pi}{c} \langle J_{\theta,j} \rangle^{M+1/2} \\ &= -\frac{4\pi}{c} \sum_{n'=0}^{n-1} W\left(n' - \frac{N}{2} \right) J_{\theta,j}(M\Delta T + n'\Delta t), \end{aligned} \tag{15}$$

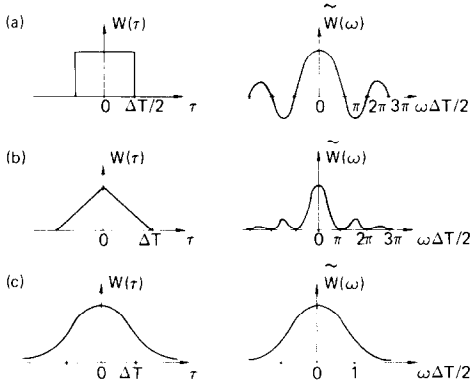

FIG. 4. Digital-smoothing function $W(t)$ as a function of time and its Fourier transform $\tilde{W}_\omega$ as a function of frequency for (a) a square data window, (b) a tent shape, and (c) a Gaussian.

where M denotes the macro time level, $N \equiv \Delta T/\Delta t$, $J_{\theta,j}$ is given by either Eq. (14a) or Eq. (14b), and a conventional centered spatial difference operator is taken for $(\partial^2/\partial r^2)$. Three illustrative examples of W and the corresponding Fourier transforms $\tilde{W}_\omega$ are shown in Fig. 4. When Eq. (14b) is used for J_θ, ψ is taken equal to $\psi^{M+1/2}$ on the right side of Eq. (14b); solution of Eq. (15) for $\psi^{M+1/2}$ is then implicit, but is straightforward. Equation (15) *predicts* the flux from which the magnetic and electric fields are then readily determined:

$$\mathbf{B}^{M+1/2} = \nabla \times \left(\frac{\psi^{M+1/2}}{r} \hat{e}_\theta \right) + \mathbf{B}_0 \tag{16}$$

and from Faraday's law,

$$E_\theta^{M+1/2} = -\frac{(1-\eta)}{\eta} E_\theta^M - \frac{2}{\eta c \Delta T} \left(\frac{\psi^{M+1/2}}{r} - \frac{\psi_M}{r} \right), \tag{17}$$

where η is a time-centering parameter. Next, particle velocities and positions are advanced forward over the N micro time steps from $t = M\Delta T$ to $t = (M+1)\Delta T$ in a *corrector* iteration using Eq. (13). The fields $(\mathbf{E}, \mathbf{B}) = (\mathbf{E}, \mathbf{B})_j''$ in Eq. (13a) are obtained by interpolation and extrapolation from $(\mathbf{E}, \mathbf{B})^M$ and the newly predicted $(\mathbf{E}, \mathbf{B})^{M+1/2}$.

With the corrected particle positions and velocities, the current $\langle J_{\theta,j} \rangle^{M+1/2}$ is accumulated again and the fields are then corrected. Ampère's law becomes

$$\left(\frac{\partial^2}{\partial r^2} - \frac{1}{r^2} \right)_j \frac{\psi^{M+1}}{r} = -\frac{(1-\alpha)}{\alpha} \left(\frac{\partial^2}{\partial r^2} - \frac{1}{r^2} \right)_j \frac{\psi^M}{r} - \frac{4\pi}{\alpha c} \langle J_{\theta,j} \rangle^{M+1/2}, \tag{18a}$$

when Eq. (14a) is used for J_θ, and

$$\left(\frac{\partial^2}{\partial r^2}-\frac{1}{r^2}\right)_j \frac{\psi^{M+1}}{r}-\frac{4\pi e^2}{mc^2}\left\langle \sum_i \frac{S(r_i^n-r_j)}{r_i^n}\right\rangle^{M+1/2} \psi_j^{M+1}$$
$$=\frac{(1-\alpha)}{\alpha}\left[\left(\frac{\partial^2}{\partial r^2}-\frac{1}{r^2}\right)_j \frac{\psi^M}{r}-\frac{4\pi e^2}{mc^2}\left\langle \sum_i \frac{S(r_i^n-r_j)}{r_i^n}\right\rangle^{M+1/2} \psi_j^M\right]$$
$$-\frac{4\pi e}{\alpha mc}\left\langle \sum_i \frac{S(r_i^n-r_j)}{r_i^n} L_{\theta,i}\right\rangle^{M+1/2} \tag{18b}$$

when Eq. (14b) is used. α is a second time-centering parameter. The magnetic and electric fields are given by

$$\mathbf{B}^{M+1}=\nabla\times\left(\frac{\psi^{M+1}}{r}\hat{e}_\theta\right)+\mathbf{B}_0 \tag{19}$$

and

$$E_\theta^{M+1}=-\frac{(1-\eta)}{\eta}E_\theta^M-\frac{1}{\eta c\Delta T}\left(\frac{\psi^{M+1}}{r}-\frac{\psi^M}{r}\right). \tag{20}$$

With $(\mathbf{E},\mathbf{B})^{M+1}$ further corrections of the particle trajectories can be made over the interval $M\Delta T\leqslant t\leqslant (M+1)\Delta T$. However, with more corrector iterations the potential economic advantage of orbit-averaging decreases. The goal of computational efficiency motivates minimizing the product of the number of simulation particles multiplied by the number of predictor–corrector iterations per macro time step that are required for stability and accuracy. In any case, after conclusion of the corrector iterations, the fields $(\mathbf{E},\mathbf{B})^{M+1}$ are used in Eq. (13) to predict new velociteis and positions over the next macro interval $(M+1)\Delta T\leqslant t\leqslant (M+2)\Delta T$. The computational cycle then continues. With appropriate extensions to five phase-space dimensions $(r, z; v_r, v_\theta, v_z)$, these equations also describe SUPERAVERAGE.

We have made available a number of different algorithm options. Our intention is to choose various options and adjust parameters in such a way as to filter out high frequencies, minimize simulation costs, and achieve numerical stability and high accuracy. The principal options and parameters at our disposal are the representation of J_θ employed, Eq. (14a) or (14b); N, the number of micro time steps per macro step; the number of corrector iterations; the values of the centering parameters α and η; the shape of the digital-smoothing function W; and the number of particles required for good statistics. In general, these selections cannot be made independently and may be somewhat dependent on the problem being studied. In the final section we summarize our preliminary simulation results and corresponding choices of options and parameter values for studies of ion-ring build-up using MAGICL and neutral-beam injection in the 2XIIB mirror plasma using SUPERAVERAGE. Our studies of the orbit-averaging method are only a beginning, but they clearly demonstrate many of the properties of the method and its power.

4. Simulation Results

We have tested one-dimensional orbit-averaged magneto-inductive codes as described in Eqs. (13) to (20) with both representations for J_θ, Eqs. (14a) and (14b). The two-dimensional code SUPERAVERAGE uses Eq. (14a) for J_θ. The algorithm making use of canonical angular momentum in J_θ, Eq. (14b), requires more storage and more operations in order to solve the resulting implicit equation for the magnetic flux. Hence this algorithm makes for a slower code, but Section 2 suggests that it may have improved numerical stability.

To provide an interesting problem for testing MAGICL and SUPERAVERAGE, parameters have been adopted to model neutral-beam driven build-up of the 2XIIB mirror plasma at Lawrence Livermore Laboratory to a high β plasma whose magnetic field is nearly reversed somewhere in the plasma [5]. In MAGICL we modeled injection by introducing deuterium ions continuously with a current $I = 50$ A/cm into a magnetic field $B_0 = 4500$ G at a radius $r = 5.5$ cm and with a spread of 1 cm. The ions had energy 12 keV injected tangent with a spread of 1.2 keV and thus encircled the axis. (The input parameters and output diagnostics of both MAGIC and MAGICL are in conventional dimensional units, but computations internal to the codes are in nondimensional scaled units [12].) In the absence of collisions and mirror losses, a 50 A/cm injection rate achieved $\Delta B/B_0 \sim 1$ after an interval of time $\omega_{ci}^0 t \sim 800$ or only a little over 125 cyclotron periods. After the magnetic field reverses, electrostatic and electron dynamical effects that are ignored in MAGIC, SUPERLAYER, and their orbit-averaged versions should be included [17]. The credibility of simulations of field reversal in the absence of these effects, as in Ref. [5], is highly suspect.

In Figs. 5 and 6 we display typical simulation results from MAGICL, with J_θ given by Eq. (14a), and MAGIC, which uses canonical angular momentum in forming J_θ. In these examples both codes used a time step $\omega_{ci}^0 \Delta t = 0.2$ and equal numbers of particles (1024). In MAGICL, $\omega_{ci}^0 \Delta T = 12.8$, so that $N = \Delta T/\Delta t = 64$, $\alpha = \eta = 0.75$, and two corrector iterations were employed. MAGIC, which was better time-centered with $\eta = 0.6$, exhibited significant noisiness in E_θ associated with the discreteness of the injection model on the micro time scale (see Fig. 6). MAGICL evidently filtered out most of this noise by averaging, time-splitting, and introducing dissipation with $\alpha, \eta > \frac{1}{2}$. We attribute the differences in the particle phase space and hence in the charge density and current to the enhanced level of E_θ oscillations in MAGIC. In the absence of these oscillations of E_θ there was a distinct ring in the $v_r - r$ phase plane (see Fig. 5). Otherwise the simulation results of the two codes bore great similarity. Figure 7 shows the results of simulations with MAGICL in which W was square-shaped in one case and smoothly switched on and off in the other. The induction electric field exhibited approximately twice the jitter for the case with the square data window but otherwise the same magnitude and trend. In all other code diagnostics it was difficult to detect any differences whatever.

Contrary to the fears expressed in Section 2, the algorithm using Eq. (14a) for J_θ performed just as well as that using Eq. (14b). No real differences in physics results,

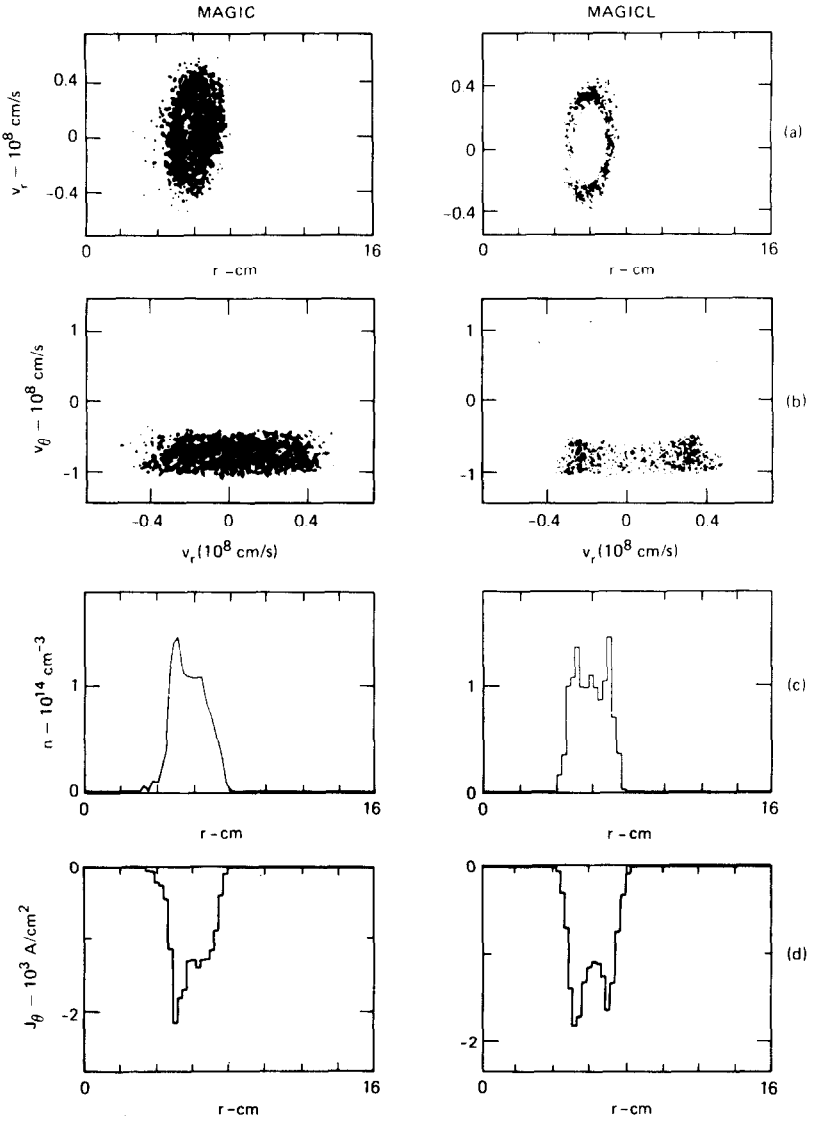

FIG. 5. Ion phase space (a) v_r vs r, (b) v_θ vs. v_r, and (c) the charge and (d) the current density profiles at $\omega_{ci}^0 t = 820$ from a simulation using MAGIC and the orbit-averaged code MAGICL with the same number of super-particles (1024). Tangential injection and buildup of a charge-neutralized deuterium current ring are studied with the following parameters: $B_0 = 4500$ G, $E_i = mv_i^2/2 = 12$ keV, $\Delta E_i/E_i = \pm 0.05$, and $I = 50$ A/cm continuously injected at $r = 5.5 \pm 0.5$ cm. There is a conducting wall at $r = 16$ cm. In MAGIC and MAGICL, $\omega_{ci}^0 \Delta t = 0.2$; in MAGICL, $\omega_{ci}^0 \Delta T = 12.8$.

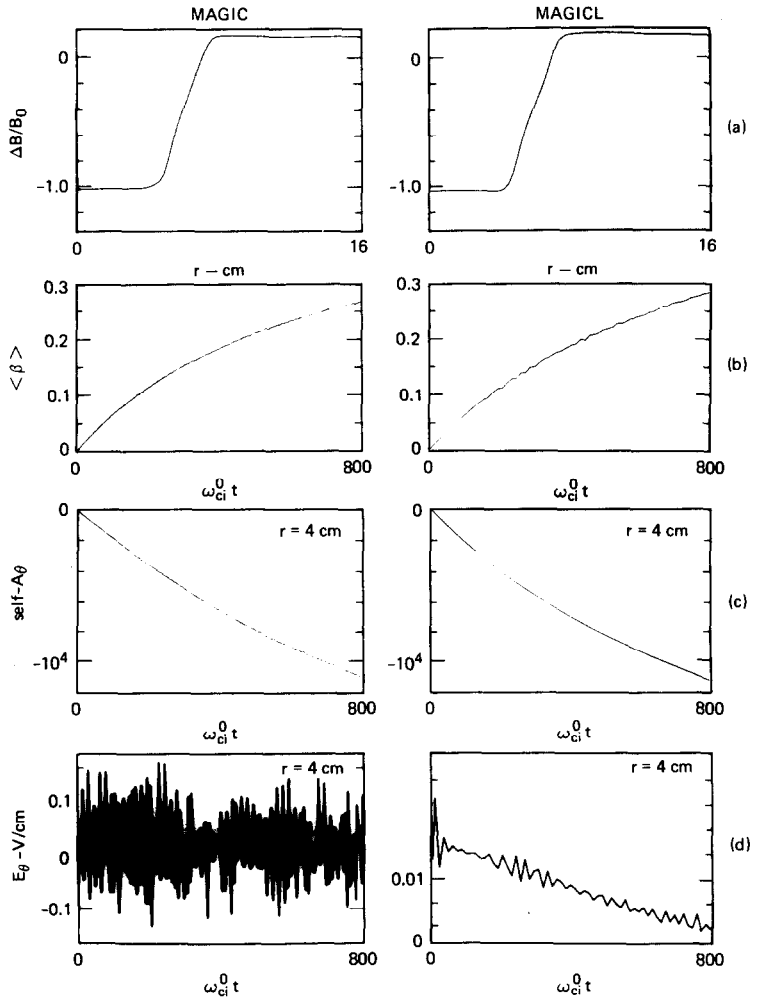

FIG. 6. For the same simulations described in Fig. 5 are shown (a) the self-magnetic field $\Delta B_z/B_0$ vs. r, (b) the spatially averaged $\beta(\beta \equiv 8\pi n m_i \langle v_i^2/2 \rangle / B_0^2)$, (c) the self-vector potential A_θ vs. $\omega_{ci}^0 t$ and (d) E_θ vs. $\omega_{ci}^0 t$.

numerical stability, and accuracy were observed. One corrector iteration was sufficient for numerical stability. However, a second corrector iteration in MAGICL reduced the relative error in the conservation of energy by a factor of 10 in some cases and to a magnitude of typically 0.1 to 0.5 %; similar results were achieved with only one corrector iteration when the interpolation/extrapolation of **E** and **B** for purposes of advancing the particles on the corrector iteration was biased backward toward the previous macro time step. Conservation of total energy and canonical momentum in MAGICL is generally quite good. Errors accumulate but can be kept

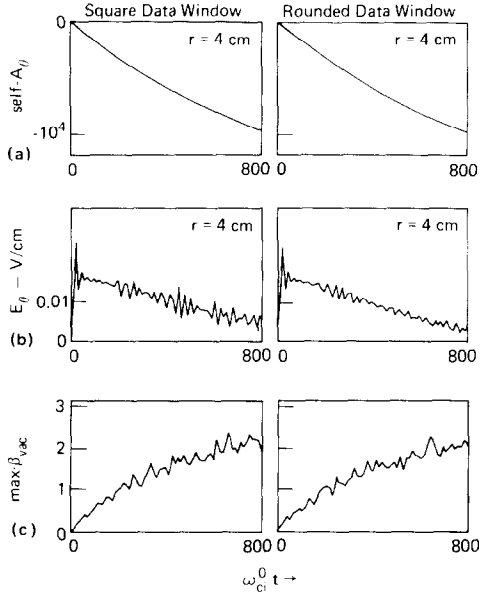

FIG. 7. For the same simulation parameters described in Fig. 5 are shown simulation results with square data window and data window switched smoothly on and off with sinusoidal time dependence: (a) A_θ vs. $\omega_{ci}^0 t$, (b) E_θ vs. $\omega_{ci}^0 t$, and (c) the maximum β in the vacuum magnetic field vs. $\omega_{ci}^0 t$. E_θ is quieter with use of the rounded data window.

at levels of less than a few percent. For $\Delta T/\Delta t \gg 1$, e.g., $\omega_{ci}^0 \Delta T > 6$, numerical stability and accuracy were independent of $\Delta T/\Delta t$, whose selection is then only restricted by just how slowly varying are the fields to be followed in the simulation. The selection of $\alpha = \eta = 0.75 \pm 0.05$ seemed to minimize energy errors and critically damped unwanted transients and high-frequency oscillations.

Extrapolation of **E** and **B** ahead in time for use in Eq. (13) in predicting new velocities made no difference compared to holding these values constant over the predictor macro time step. Use of second-order interpolation and extrapolation of **E** and **B** in time to advance the velocities on the corrector iteration resulted in no significant improvement over first-order interpolation and extrapolation. However, holding **E** and **B** constant in time during both corrector and predictor iterations led to unacceptable particle trajectories. This was due to the resulting "jerks" when at each macro time step **E** and **B** changed by discrete amounts, but were constant over all intervening micro time steps. We have observed that significant quieting of E_θ noise arising from the discreteness of the injection model occurred in simulations with MAGICL. This represents a real improvement in bringing the physics model closer to rality. As previously mentioned, a rounded digital-smoothing function W further reduced noise in E_θ, but not dramatically.

For our one-dimensional studies of build-up to near field reversal with the injection rate held constant, we were able to reduce the particle requirement by a factor of 2 with orbit-averaging. Because the injection was tangential and at a distance approx-

imately equal to the ions' Larmor radii, ring-like plasmas were produced in these studies. Systems with such high degrees of order can be simulated without aid of orbit-averaging with fairly few particles, ~1000 in our studies; therefore not much reduction can be obtained with orbit-averaging. With increased disorder and a slower injection rate, so that $|d \ln B/dt|$ was correspondingly smaller, we were able to employ a larger ratio of $\Delta T/\Delta t$ and fewer particles than in a conventional simulation. We thus have evidence that the economic success of the application of orbit-averaging to magneto-inductive simulation is dependent on the particular problem, while numerical stability and a good accuracy were not.

We speculate that the use of orbit-averaging in a simulation with a high intrinsic statistical requirement offers greater likelihood of gain in computational efficiency, say, for example, in electrostatic simulations of warm plasmas in which charge separation and Debye shielding effects must be adequately resolved. We already have evidence that the savings of particles and hence in computations can be more substantial in a magneto-inductive simulation of a plasma with a significant degree of disorder and with an increased number of phase-space dimensions. In simulations of diffuse injection and build-up of the 2XIIB mirror experiment with SUPERAVERAGE, which has five phase-space dimensions $(r, z; v_\theta, v_r, v_z)$, orbit averaging has enabled the reduction of the particle requirement by a factor of 16 relative to previous SUPERLAYER simulations in some cases. Furthermore, these simulations were stable and exhibited less than 1 % discrepancy in energy conservation with only one corrector iteration, which made for a total of two passes through the particle mover per time step Δt. Thus there was achieved a reduction by $16/2 = 8$ in computations associated with particle-pushing through the use of orbit-averaging in some of our simulations.

Figures 8 and 9 show simulation results from SUPERAVERAGE and COMPARABLE results from SUPERLAYER. Deuterium atoms were injected continuously at a rate $I = 300$ A with a bimodal energy spectrum peaked at 14 and 10 keV. These neutrals were ionized by electron collisions and charge exchange in a target plasma with presumed electron temperature of 50 eV. Ions were deposited diffusely over a radius $0 \leqslant r \leqslant 7.5$ cm and an axial extent $-20 \text{ cm} \lesssim z \lesssim 20$ cm. The applied magnetic field was 4350 G in the midplane with a mirror ratio of 1.2 at $z = \pm 50$ cm. The self-magnetic fields grew to $\Delta B/B_0 \sim 0.7$ at steady state, and the density built up to $n = 2 \times 10^{14} \text{ cm}^{-3}$. For the simulation with SUPERAVERAGE $\omega_{ci}^0 \Delta t = 0.2$, $\Delta T/\Delta t = 60$, one corrector iteration was used, $\alpha = \eta = 0.95$, and there was a sixteenfold reduction in the injection rate of simulation particles but no reduction in the total current represented. These values of α and η differ slightly from the optimal values used in MAGICL. The optimal values of α and η were somewhat problem dependent, and best results were obtained in MAGICL by tuning the choice of α and η for the particular type of problem involved. Similar tuning has so far not been performed in SUPERAVERAGE. The SUPERAVERAGE simulation results agreed with those of SUPERLAYER within reasonable expectations, but quite effectively filtered noise associated with the discreteness of the injection model, and hence were much quieter.

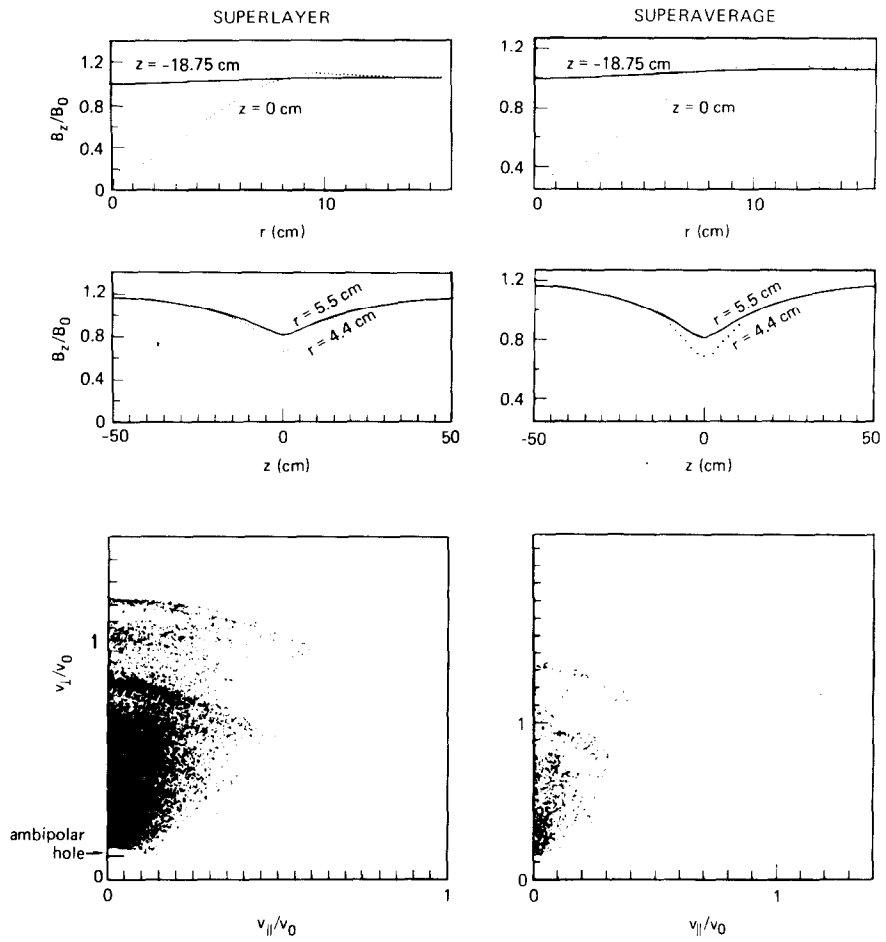

FIG. 8. Simulations with SUPERLAYER and SUPERAVERAGE of neutral-beam (deuterium) injection at rate 300 A into an applied magnetic field of $B_0 = 4350$ G at the midplane with mirror ratio 1.2 at $z = \pm 50$ cm. The neutrals had 12 keV average energy and were deposited diffusely over $0 \leqslant r \leqslant 7.5$ cm and -20 cm $\leqslant z \leqslant 20$ cm. The simulations used $\omega_{ci}^0 \Delta t = 0.2$ and included ion drag on electrons. In SUPERAVERAGE, $\Delta T/\Delta t = 60$ and only one corrector iteration was used. At nearly steady state ($\omega_{ci}^0 t = 120$) are shown B_z/B_0 vs. radius r and axial position z, and the ion phase space v_r/v_0 vs. $v_{||}/v_0$, where v_0 is the velocity corresponding to the average injection energy of 12 keV.

We are particularly enthusiastic over the orbit-averaging technique, because it is now feasible to simulate mirror plasmas like the 2XIIB experiment without artificially accelerating the classical and anomalous diffusion rates and the neutral-beam injection and deposition rates, which had heretofore implied an arbitrary compression of the difference in build-up/transport and ion cyclotron time scales. In one preliminary case with SUPERAVERAGE, we employed a reduction of ~6000 in the

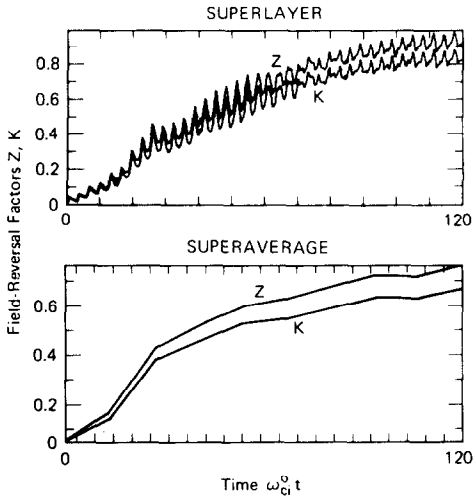

FIG. 9. For the simulations described in Fig. 8 are shown the maximum $Z \equiv 1 - (B_z)_{\min}/(B_z)_{\max}$ and $K \equiv 1 - (B_z)_{\min}/B_0$ in the midplane $(z = 0)$ as functions of time. The oscillations in the SUPERLAYER Z and K traces coincide with the discrete pulses of newly injected ions. These pulses drove oscillations in E_θ, which modified in turn the ion orbits and were responsible for the oscillatory and systematic differences in Z and K obtained with SUPERLAYER and SUPERAVERAGE.

injection rate with respect to SUPERLAYER which had accelerated this rate. This simulation had $\lesssim$650 particles in it at steady state, as compared to the ~20,000 particles that were typically required in a conventional simulation. Furthermore, there was no acceleration of the classical ion-electron slowing-down rate $\nu_s^{i/e}$ relative to the ion cyclotron frequency for the parameters used in the simulation to model the 2XIIB experiment. For a density of ionized deuterium $n_0 \sim 2 \times 10^{14}$ cm^{-3} at steady state, an assumed electron temperature $T_e = 55$ eV, and $B_0 = 4350$ G, $\omega_{ci}^0 t = 2.4 \times 10^4$ and $\nu_s^{i/e} t = 6$ at the end of the simulation. This simulation required 34 minutes on the CRAY I computer. Orbit-averaging and time-splitting have thus allowed us to begin simulating efficiently and accurately a magnetic fusion experiment of current interest without artificial acceleration of slow time scales and rescaling of fundamental plasma parameters.

ACKNOWLEDGMENTS

We are grateful to Jack Byers for initially stimulating interest in this endeavor and for his continuing assistance and encouragement. We also thank A. B. Langdon, C. K. Birdsall, W. C. Condit, and A. Friedman for a number of valuable discussions, suggestions, criticisms, and interest.

This work was performed under the auspices of the U.S. Department of Energy by the Lawrence Livermore Laboratory under Contract W-7405-ENG-48.

REFERENCES

1. C. K. BIRDSALL AND A. B. LANGDON, Plasma physics via computer simulation, to be published.
2. J. A. BYERS, B. I. COHEN, W. C. CONDIT, AND J. D. HANSON, *J. Computational Phys.* **27** (1978), 363; A. FRIEDMAN, R. L. FERCH, R. N. SUDAN, AND A. T. DROBOT, *Plasma Phys.* **19** (1977), 1101.
3. J. A. BYERS, private communication.
4. R. P. FREIS, *Nucl. Fusion* **13** (1973), 247.
5. J. A. BYERS, *Phys. Rev. Lett.* **39** (1977), 1476.
6. B. B. GODFREY, *J. Computational Phys.* **15** (1974), 504.
7. A. B. LANGDON AND B. F. LASINSKI, *in* "Methods in Computational Physics" (J. Killeen, Ed.), Vol. 16, p. 338, Academic Press, New York, 1976.
8. C. E. RATHMANN, J. L. VOMVORIDIS, AND J. DENAVIT, *J. Computational Phys.* **26** (1977), 408.
9. T. L. CRYSTAL, J. DENAVIT, AND C. E. RATHMANN, *Comments Plasma Phys. Cont. Fusion* **5** (1979), 17.
10. A. B. LANGDON, *J. Computational Phys.* **30** (1979), 202.
11. D. O. DICKMAN, R. L. MORSE, AND C. W. NIELSON, *Phys. Fluids* **12** (1969), 1708.
12. T. A. BRENGLE AND B. I. COHEN, "MAGIC: A One-Dimensional Magneto-Inductive Particle Code," Lawrence Livermore Laboratory Report UCID-17795 Rev. 1, University of California, July 1978.
13. C. G. DARWIN, *Philos. Mag.* **39** (1920), 537; C. W. NIELSON AND H. R. LEWIS, *in* "Methods in Computational Physics" (J. Killeen, Ed.), Vol. 16, p. 367, Academic Press, New York, 1976.
14. J. P. BORIS, *in* "Proceedings of the Fourth Conference on Numerical Simulation of Plasma" (J. P. Boris and R. Shanny, Eds.), p. 3, U.S. Government Printing Office, Washington, D.C., 1971.
15. D. FUSS AND C. K. BIRDSALL, *J. Computational Phys.* **3** (1969), 494.
16. A. FRIEDMAN AND R. L. FERCH, private communication.
17. D. E. BALDWIN AND M. E. RENSINK, *Comments Plasma Phys. Cont. Fusion* **4** (1978), 55.